Journal of Neuroimmunology 330 (2019) 96–107

Contents lists available at ScienceDirect

Journal of Neuroimmunology

journal homepage: www.elsevier.com/locate/jneuroim

Effect of cornel iridoid glycoside on microglia activation through suppression of the JAK/STAT signalling pathway

Zhao Qu[a,b,1], Na Zheng[a,b,1], Yuzhen Wei[c,d,1], Yujing Chen[a], Yifan Zhang[a,b], Ming Zhang[a], Haoxiao Chang[a], Jianghong Liu[a], Houxi Ai[a], Xingchao Geng[e,*], Qi Wang[b,*], Linlin Yin[a,c,d,*]

[a] Xuan Wu Hospital of Capital Medical University, 45 Changchun Street, Beijing 100053, PR China
[b] Institute of Clinical Pharmacology, Guangzhou University of Chinese Medicine, 12 Jichang Road, Guangzhou, Guangdong Province 510405, PR China
[c] Department of Neurology, Beijing Tiantan Hospital, Capital Medical University, Beijing, China
[d] China National Clinical Research Center for Neurological Diseases, China
[e] National Center for Safety Evaluation of Drugs, National Institute for Food and Drug Control, Beijing 100176, PR China

ARTICLE INFO

Keywords:
Microglia
Cornel iridoid glycoside
Neuroinflammation
JAK/STAT pathway

ABSTRACT

The effect of cornel iridoid glycoside (CIG), main component extracted from *Cornus officinalis*, on microglia activation has not been elucidated so far. We induced a mouse model of multiple sclerosis (MS), namely, the experimental autoimmune encephalomyelitis (EAE) model by immunization subcutaneously with the $MOG_{35–55}$ peptide, which causes neuroinflammation and microglia activation. Our data demonstrated that CIG delayed the onset of the EAE, ameliorated the severity of the symptoms and inhibited the activation of microglia in different brain regions. In addition, we also found that CIG has therapeutic potential by modulating microglia polarization by reducing the expression and release of proinflammatory cytokines, chemokines and inhibiting phosphorylation in the JAK/STAT cell signalling pathway. Based on our findings, CIG might be a promising candidate for the prevention of neurological disorders such as multiple sclerosis (MS).

1. Introduction

Multiple sclerosis (MS) is an autoimmune disease of the central nervous system (CNS) characterized by demyelination, inflammatory lesions, activation of Th1 and Th17 cells, inappropriate activation of innate immune cells such as microglia, and aberrant production of cytokines/chemokines (Qin et al., 2010). The pathogenesis of MS and its animal model, experimental autoimmune encephalomyelitis (EAE), is associated with microglia activation (O'Loughlin et al., 2018; Yin et al., 2014). Microglias are resident immune cells in the central nervous system. In the resting state, microglia move constantly in the brain, exchange molecular signals by synaptic interactions, and phagocytose damaged neurons. Upon stress or brain damage, microglia are activated and involved in neuronal recovery (Tremblay et al., 2011). However, persistent microglia activation produces various inflammatory and neurotoxic molecules and leads to neuronal cell death (Gao and Tsirka, 2011; Harry, 2013; Rawji and Yong, 2013). Thus, controlling microglia activation has been suggested as an important therapeutic strategy for various neuroinflammatory disorders such as Alzheimer's disease, Parkinson's disease, and MS.

The JAK/STAT signalling pathway is used by numerous cytokines and is critical for initiating innate immunity, orchestrating adaptive immunity, and ultimately constraining immune responses (O'Shea and Plenge, 2012). There is evidence for aberrant functionality of the JAK/STAT pathway in MS and EAE. Ahn et al. (2017) report that glial STAT1 and STAT3 are distinctively phosphorylated following the interaction of activated lymphocytes and glia, and this effect is significantly inhibited by glatiramer acetate (GA), a disease-modifying drug for MS. GA also reduces the activation of STAT1 and STAT3 by MS-associated stimuli such as IFN-γ or LPS in the primary glia. In EAE, IL-6 has a deleterious role by activating STAT3 (Benveniste et al., 2014), JAK inhibitor reduced the severity of EAE (Liu et al., 2014). Thus, unrestrained activation of the JAK/STAT pathway has pathological implications for MS.

Cornus officinalis is a member of the Cornaceae family. This herb was first recorded in Shen Nong's Materia Medica approximately 2000 years ago in China and is often used to tonify the liver and the kidney according to the theory of traditional Chinese medicine. Cornel iridoid glycoside (CIG) is the main component extracted from *Fructus Corni*. Previous studies in our laboratory found that the JAK/STAT signalling pathway is involved in the effect of CIG on rats with EAE (Yin

* Corresponding authors at: Xuan Wu Hospital of Capital Medical University, 45 Changchun Street, Beijing 100053, PR China.
E-mail addresses: cyj0504@sina.com.cn (Y. Chen), gengxch@nicpbp.org.cn (X. Geng), wangqi@gzhtcm.edu.com (Q. Wang), yinlinlin@bjtth.org (L. Yin).
[1] Both authors contributed equally to this study.

https://doi.org/10.1016/j.jneuroim.2019.01.014
Received 7 September 2018; Received in revised form 24 January 2019; Accepted 24 January 2019

et al., 2014). However, the role of CIG in microglia activation has not been clearly demonstrated until now. Therefore, in the present study, we examined not only the beneficial effect of CIG on MOG-EAE but also the effect of CIG on LPS/IFN-γ- or IL-4/IL-10-stimulated microglia polarization. In addition, the molecular mechanisms underlying the effect of CIG were analysed with a focus on the possible mechanisms modifying the JAK/STAT signalling pathway.

2. Materials and methods

2.1. Animals

Female C57BL/6J mice aged 7 weeks (weighing between 18 and 20 g) were purchased from Beijing Vital River Laboratory Animal Technology, Co. Ltd. (Beijing, China) and were housed in a 12/12 h light/dark cycle and specific pathogen-free (SPF) conditions with laboratory chow and water ad libitum. All experiments were performed in compliance with National Institutes of Health (NIH) guidelines for the Care and Use of Laboratory Animals, reviewed and approved by the Bioethics Committee of Xuan Wu Hospital of Capital Medical University.

2.2. Materials

The sarcocarp of *C. officinalis* was purchased from the Tong-Ren-Tang Company, Beijing, China. CIG was extracted from *C. officinalis* as described previously (Yao et al., 2009). The purity of CIG was 71.19%, as determined by high-performance liquid chromatography, in which morroniside accounted for 67% and loganin 33%. The myelin oligodendrocyte glycoprotein peptide (MOG) 35–55 (MEVGWYRSPFSRVVHLYRNGK) was synthesized by Beijing Scilight Biotechnology Ltd. Co (purity > 98%). Complete Freund's adjuvant (CFA) containing *Mycobacterium tuberculosis* H37Ra was purchased from Difco, while interferon-γ (IFN-γ) and *Bordetella pertussis* toxin were from R&D. Lipopolysaccharide (LPS) and β-actin antibody were from Sigma-Aldrich Co. Unless otherwise specified, all the other reagents were from Sigma-Aldrich Co.

2.3. EAE induction and drug treatment

The protocol for EAE induction was carried out according to Stromnes and Goverman (2006). Mice were divided randomly into the following 4 groups: control, $MOG_{35–55}$-treated, and $MOG_{35–55}$-treated with CIG (50 or 100 mg/kg) groups. Briefly, 2 mg/ml of $MOG_{35–55}$ peptide in PBS were emulsified 1:1 in complete Freund's adjuvant supplemented with 4 mg/ml *Mycobacterium tuberculosis*; 200 μl of emulsion containing 200 μg of $MOG_{35–55}$ were injected s.c. into 3–4 different locations on the backs of female C57BL/6J mice. Additionally, 500 ng of pertussis toxin (PTX) in PBS were administered i.p. on days 0 and 2. Meanwhile, the mice of control group were immunized with vehicle without $MOG_{35–55}$ peptide. An identical booster was given in the other flank 1 week later (Gilgun-Sherki et al., 2003). Following the encephalitogenic challenge, mice were observed daily after booster and clinical-behavioural manifestations of EAE were scored as follows: 0 = no clinical symptoms; 1 = loss of tail tonicity; 2 = partial hind limb paralysis; 3 = complete hind limb paralysis; 4 = paralysis of four limbs; 5 = total paralysis; 6 = death (Mendel et al., 1998).

Daily treatment with vehicle or CIG (50 or 100 mg/kg) was started at day 0 intragastrically 2 h after daily monitoring and continued to day 24 post-immunization. The volume of the gastrointestinal treatment was 10 ml/kg. Animals in the control group received equal volumes of saline by the same route.

2.4. Cell cultures

The murine microglia cell lines BV2 and N9 were kindly provided by Prof. Yumin Luo (Cerebrovascular Diseases Research Institute and Department of Neurosurgery, Xuan Wu Hospital of Capital Medical University). BV2 and N9 cells were cultured in RPMI 1640 (Gibco) and Dulbecco's modified Eagle's medium (DMEM)/F12 medium (Gibco) respectively, supplemented with 10% Foetal Bovine Serum (FBS, Gibco), 100 U/mL penicillin and 100 μg/mL streptomycin (Gibco) and were maintained at 37 °C, 95% air and 5% CO_2 in a humidified incubator. Cells were pretreated in the absence or presence of CIG (25, 50, 100 and 200 μg/mL) for 30 min and then stimulated with LPS (100 ng/mL) and IFN-γ (10 ng/mL) for 24 h.

2.5. Immunohistochemistry

All mice were sacrificed on day 25 after $MOG_{35–55}$ immunization. Animals were anaesthetized with chloral hydrate (400 mg/kg) by intraperitoneal injection and perfused intracardially with normal saline followed by 4% paraformaldehyde (PFA) in phosphate buffer (3.12 g/L of NaH_2PO_4, 28.64 g/L of Na_2HPO_4•$12H_2O$, 30 g/L sucrose, pH -7.4) for fixation. The whole brain was removed and post-fixed in 4% PFA in phosphate buffer saline (PBS) at 4 °C overnight, followed by cryoprotection in 30% sucrose in PBS for 3 days. Tissues were cut coronally in 40 μm serial frozen sections using a Thermo cryostat.

For immunohistochemistry, free-floating sections were incubated with 3% hydrogen peroxide for 10 min to quench endogenous peroxide activity, then blocked with 10% normal goat serum in 0.01 M PBS containing 0.01% Triton X-100 (PBS-T) for 1 h at 37 °C and incubated for 48 h at 4 °C with a rabbit anti-ionized calcium binding adaptor molecule 1 (Iba-1, dilution 1:500; Wako), which was used as a marker for microglia. Sections were then incubated with biotinylated secondary goat anti-rabbit antibody (dilution 1:200, ZSGB-BIO), followed by avidin-biotin peroxidase complex. A final incubation in diaminobenzidine was performed for visualization. All sections were washed in PBS, mounted on aminopropyl triethoxysilane-coated slides, dried, dehydrated in a graded series of ethanol, cleared in xylene, and cover slipped with DPX.

2.6. Detection of cytokines and nitric oxide levels

BV2 microglia cells (1×10^5 cells per well in a 24-well plate) were pretreated with CIG for 30 min and stimulated with LPS (100 ng/mL) and IFN-γ (10 ng/mL). The supernatants of the cultured microglia were collected 24 h after LPS/IFN-γ stimulation and the concentrations of IL-1β (R&D), IL-6 (eBioscience) were measured by an enzyme-linked immunosorbent assay (ELISA). Accumulated nitric oxide was measured in the cell supernatant using the Griess reagent (Promega). Data are represented as pg/mL or mg/mL and all samples were measured in duplicate.

2.7. RNA isolation, RT-PCR, and real-time PCR

BV2 cells (5×10^5 cells in 60 mm dish) were treated with LPS/IFN-γ in the presence or absence of CIG, and total RNA was extracted with TRIzol (Takara) according to the manufacturer's instructions. For RT-PCR, total RNA (1 μg) was reverse transcribed into cDNA with PrimeScript™ RT reagent Kit with gDNA Eraser (Takara) according to the manufacturer's instructions. The synthesized cDNA was used as a template for PCR reactions and the primers are shown in Table 1.

Real time RT-PCR was described previously (Ogata et al., 2006). The SYBR® Premix Ex Taq™ II (Tli RNaseH Plus), ROX plus (Takara Biotech) was used for the detection of the target genes: 95 °C for 5 s, 60 °C for 40 s, followed by 45 cycles. The comparative threshold cycle method and an internal control (β-actin) were used to normalize the expression of the target genes. To prove that the cDNA of cytokines and β-actin were amplified with the same efficacy, a standard curve was made where the Ct values were plotted against cDNA concentration.

Table 1
Real-time PCR primers.

	Forward primer	Reverse primer	Size (bp)
TNF-α	5′CTCTGTGAAGGGAATGGGTG3′	5′GGGCTCTGAGGAGTAGACGATAAAG3′	94
IL-6	5′TCCTACCCCAATTTCCAATGCTCT3′	5′ACCACAGTGAGGAATGTCCACAA3′	189
IFN-γ	5′TAACTCAAGTGGCATAGATGTGGAAG3′	5′GACGCTTATGTTGTTGCTGATGG3′	169
MCP-1	5′GAAGCTGTAGTTTTTGTCACCAAGC3′	5′GGTTCCGATCCAGGTTTTTAATGT3′	97
IL-4	5′TCGTCTGTAGGGCTTCCAAGGTGCT3′	5′GTGGACTTGGACTCATTCATGGTGC3′	166
IL-10	5′CTGGACAACATACTGCTAACCGACTC3′	5′AACTGGATCATTTCCGATAAGGC3′	86
IL-12p40	5′TCAACGCAGCACTTCAGAATCACAA3′	5′GAAGGCGTGAAGCAGGATGCAGAGC3′	185
IL-12p70	5′ACTCCCCATTCCTACTTCTCCCT3′	5′CACTTGCTGCATGAGGAATTGTA3′	197
β-Actin	5′GCCTTCCTTCTTGGGTAT3′	5′GGCATAGAGGTCTTTACGG3′	97

2.8. Western blotting

Microglia BV2 cells (5×10^5 cells/mL seeded in 60 mm dishes) were pretreated with CIG (25, 50, 100 and 200 μg/mL) for 30 min and stimulated by LPS (100 ng/mL) and IFN-γ (10 ng/mL) for 24 h. Cell pellets were harvested, washed with PBS twice (4 °C, pH 7.4), then re-suspended in lysis buffer (Tris 10 mM pH 7.5, NaCl 130 mM, Triton X-100 1%, NaF 1 mM, sodium orthophosphate (NaPi) 10 mM, sodium pyrophosphate (NaPPi) 10 mM, and phenylmethylsulfonyl fluoride (PMSF) 1 mM) containing protease inhibitor cocktail. Cell lysates with 20–40 μg of protein/lane were subjected to sodium dodecyl sulfate (SDS)-PAGE in acrylamide mini-gels and then blotted onto nitrocellulose membranes (Hybond America). Membranes were blocked with Tris-buffered saline containing 0.1% Tween-20 and 5% non-fat milk (TBST/5% milk) and then incubated overnight with primary antibodies in TBST/5% milk at 4 °C. Membranes were then washed with TBST and incubated for 1 or 2 h in TBST/5% milk containing a horseradish peroxidase (HRP)-conjugated secondary antibodies (1:2000). After washing in TBST, enhanced chemiluminescence detection (Millipore) was used to visualize the HRP-coated bands. Images were captured through a Charge Coupled Device camera, and gel bands were analysed using the GIS 1D gel Image System Version 3.73 (Tanon, Shanghai, China). The following primary antibodies were used in this study: rabbit monoclonal anti-Jak1 (1:1000, Epitomics), rabbit polyclonal anti-phospho-Jak1 (1:500, Millipore), rabbit polyclonal anti-Jak3 (1:200, Abcam), rabbit monoclonal anti-phospho-Jak3 (1:1000, Epitomics), rabbit monoclonal anti-STAT1 (1:1000, Epitomics), mouse monoclonal anti-phospho-Tyr 701 of STAT1 (1:1000, CST), rabbit monoclonal anti-phospho-Ser 727 of STAT1 (1:1000, Epitomics), rabbit monoclonal anti-STAT3 (1:1000, Epitomics), rabbit monoclonal anti-phospho-Tyr 705 of STAT3 (1:1000, Epitomics), rabbit polyclonal anti-phospho-Ser 727 of STAT3 (1:1000, Abcam), rabbit polyclonal anti-SOCS1 (1:1000, CST), rabbit polyclonal anti-iNOS (1:1000, Abcam), rabbit polyclonal anti-COX-2 (1:1000, CST), rabbit polyclonal NF-κB (1:1000, CST), goat polyclonal anti-ICAM-1 (1:1000, R&D), rabbit polyclonal anti-IL-6Rα (1:1000, Abcam), rabbit polyclonal anti-gp130 (1:1000, Abcam), mouse monoclonal anti-β-actin (dilution 1:2000, Sigma). Horseradish peroxidase (HRP)-conjugated secondary antibodies (1:2000) were from Abcam.

2.9. Immunofluorescence staining

BV2 cells (1×10^5 cells/mL per well in a 48-well plate) were incubated with or without LPS (100 ng/mL) and IFN-γ (10 ng/mL) followed the pretreatment of CIG (25, 50, 100, 200 μg/mL) for 30 min. The cells were fixed with 4% formaldehyde, permeabilized with 0.1% Triton X-100 for 10 min, and then blocked in PBS containing with 5% donkey serum. Cells were incubated with rat anti-mouse CD16 antibody (1:400, BD Biosciences) or anti-mouse CD206 antibody (1:500, BD Biosciences) at 4 °C overnight followed by Alexa Fluor 594-conjugated donkey anti-mouse IgG (1:400, Life Technologies) for 2 h. Images were captured using a fluorescence microscope (Olympus) and analysed using Image-ProPlus 6.0 software (Media Cybernetics, Inc., Bethesda, USA).

2.10. Immunofluorescent confocal microscopy

Murine N9 cells (1×10^4 cells/mL per well in a 24-well plate) incubated with Alexa Fluor 488-conjugated LPS or Alexa Fluor 594-conjugated IFN-γ in the presence or absence of CIG (100 μg/mL) or minocycline (20 μM) for 24 h. The cells were then fixed with 4% formaldehyde, permeabilized with 0.2% Triton X-100 for 10 min, and then washed twice with PBS. The cells were incubated with DAPI (Life Tech.) for 5 min. Images were observed by confocal microscopy (Olympus). Antibodies Alex Fluor 488-conjugated LPS (1:100) and Alexa Fluor 594-conjugated IFN-γ (1:500) were from Life Technologies.

2.11. Statistical analysis

Experimental values are expressed as the mean ± standard error of mean (SEM). Statistical differences between groups were analysed by one-way analysis of variance (ANOVA) followed by Student–Newman–Keuls post hoc or Turkey's tests. Difference was considered statistically significant at $P < .05$.

3. Results

3.1. Effect of CIG on the severity of neurological deficits in the EAE mice

Mice were inoculated with the $MOG_{35–55}$ peptide to induce EAE. As illustrated in Fig. 1, compared with the EAE group, CIG administration

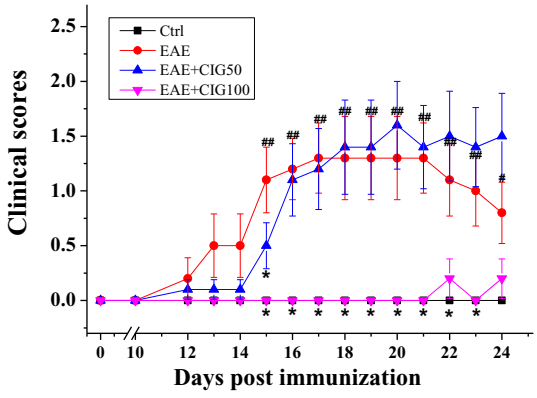

Fig. 1. Attenuation of EAE by cornel iridoid glycoside (CIG) treatment. Female C57BL/6 mice were immunized with myelin oligodendrocyte $glycoprotein_{35–55}$ ($MOG_{35–55}$, 200 μg) emulsified in complete Freund's adjuvant (CFA) containing 4 mg *Mycobacterium tuberculosis* (strain H37RA, Difco). Clinical scores of neurological deficits post-immunization up to 24 days are shown. Data are presented as the mean ± SEM ($n = 10$ per group). $^{*}P < .05$ for CIG-treated mice versus EAE mice (model group), $^{\#}P < .05$, $^{\#\#}P < .01$ for EAE mice versus control mice.

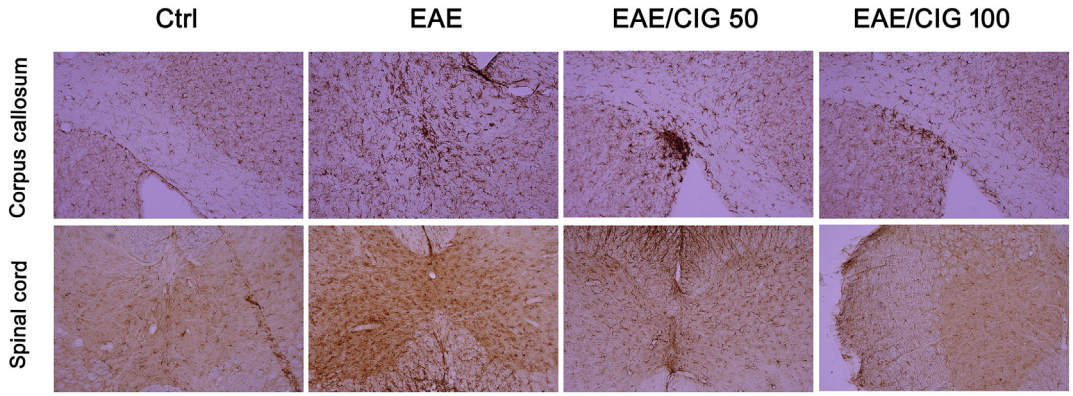

Fig. 2. Effect of cornel iridoid glycoside (CIG) on the activation of microglia (Iba-labelled). Representative photographs of the Iba-1 positive cells in the corpus callosum and spinal cord are presented. Sections are from at least 3–4 mice (4 sections per mouse). Scale bar, 100 μm.

resulted in a significant reduction in clinical scores. Our results demonstrated that 90% of the mice in the EAE group developed severe neurological deficits on day 12 after immunization, while only 70% of the EAE + CIG 50 group or 20% of the EAE + CIG 100 group showed mild neurological deficits with a delay of disease onset to day 15 and day 21, respectively. Correspondingly, CIG (50, 100 mg/kg) markedly decreased the severity of neurological deficit in a dose-dependent manner with a clinical score of 0.50 ± 0.21, 0.0 ± 0.0, respectively, when compared with 1.10 ± 0.30 in the EAE group on day 15 post-immunization when neurological deficits reached a peak.

3.2. CIG inhibited activation of microglia in the corpus callosum and spinal cord of EAE mice

Consistent with previous studies, vehicle-treated EAE mice exhibited increases in Iba-1 immunostaining. A marked decrease in microglia activation by histological analysis of cortex was observed after CIG administration (50 and 100 mg/kg). As shown in Fig. 2, the immunohistochemical results showed a decreased infiltration of microglia (Iba-1 labelled) staining in cells in the corpus callosum and spinal cord of CIG-treated mice.

3.3. Effect of CIG on microglia polarization

Microglias with different phenotypes have distinct impacts on the survival and differentiation of oligodendrocyte lineage cells (Miron et al., 2013). For example, M1 microglias are characterized by proinflammatory effects and lead to exacerbation of tissue damage, whereas M2 microglia resolve local inflammation and facilitate tissue repair (Hu et al., 2015). As shown in Fig. 3A and B, BV2 cells were treated with or without CIG (25, 50, 100 and 200 μg/mL) for 24 h before stimulation with LPS (100 ng/mL) and IFN-γ (10 ng/mL) for 30 min. We found that CIG treatment (25–200 μg/mL) significantly reduced LPS/IFN-γ-induced CD16 staining, a marker for M1 microglia polarization, in a dose-dependent manner. Meanwhile, without LPS/IFN-γ stimulation, the control group showed no M1 polarization. This finding suggests that CIG inhibits microglia polarization towards the M1 phenotype.

Here, we further tested whether CIG could modulate the microglial M2 phenotype during the recovery phase. As shown in Fig. 3C and D, Iba-1 immunostaining revealed microglial activation, and IL-4/IL-10 induction increased M2 microglia (CD206 labelled). CIG pretreatment increased or maintained the number of M2 microglia. Collectively, these findings suggest that CIG promotes microglial polarization to the beneficial M2 phenotype.

3.4. CIG suppressed iNOS expression

It is well known that inducible nitric oxide synthase (iNOS) is a major effector of innate immune signalling (Meng et al., 2016), and in association with other inflammatory mediators, iNOS serves as a marker indicating M1 microglia polarization and plays an important role in inflammation. As shown in Fig. 4A, B the BV2 cells were treated with or without CIG (25, 50, 100 and 200 μg/mL) for 24 h before stimulation with or without LPS (100 ng/mL) and IFN-γ (10 ng/mL) for 30 min. We found that CIG treatment (100, 200 μg/mL) significantly reduced LPS/IFN-γ-induced iNOS staining, another marker for M1 microglia polarization, in a dose-dependent manner. Meanwhile, immunoblotting revealed that CIG inhibited the proteins of iNOS expression (Fig. 4C).

3.5. CIG inhibited IL-6 and NO levels in BV2 microglia cells

The BV2 cells were treated with CIG for 30 min before stimulation with LPS/IFN-γ, and the effects of CIG on the LPS/IFN-γ-induced production of cytokines and NO were examined. As shown in Fig. 5B and C, CIG significantly inhibited IL-6 and NO production in the LPS/IFN-γ-induced BV2 cells; however, CIG did not affect IL-1β levels (Fig. 5A).

3.6. CIG inhibited the expression of cytokine mRNA

It is also well known that the overproduction of these proinflammatory mediators contributes to the development and progression of various diseases (Jung et al., 2013).

Total RNA was extracted from the BV2 cells, which were treated with LPS/IFN-γ in the presence or absence of CIG. For real-time PCR, relative mRNA levels of the indicated genes are shown in Fig. 6. Pretreatment with CIG (25–200 μg/mL) could prevent the induction of TNF-α, IFN-γ, IL-6, MCP-1, IL-12 (p35) and IL-12 (p40) mRNA expression. IL-4 mRNA expression was significantly promoted by CIG pretreatment. CIG pretreatment induced an increase in IL-10 mRNA expression without significance.

3.7. CIG inhibited the JAK/STAT pathway in the BV2 microglia cells

Many cytokines, such as IFN-γ, are important in activating macrophages and use the JAK/STAT pathway for signalling (O'Shea and Plenge, 2012; Qin et al., 2012a). STAT1 and STAT3 are important transcription factors in the immune response and play roles in the inflammatory signalling cascades triggered by LPS, IFN-γ, and other cytokines. As shown in Fig. 7A & B, LPS/IFN-γ stimulation led to increased STAT1 and STAT3 tyrosine phosphorylation, which was inhibited by CIG treatment in a dose-dependent manner. We further examined the effect of CIG on upstream JAK activation. LPS/IFN-γ induced a significant JAK1 and JAK3 phosphorylation, and CIG pretreatment inhibited the phosphorylation of both JAK1 and JAK3 (Fig. 8). These data indicate that CIG has a direct inhibitory effect on the JAK/STAT

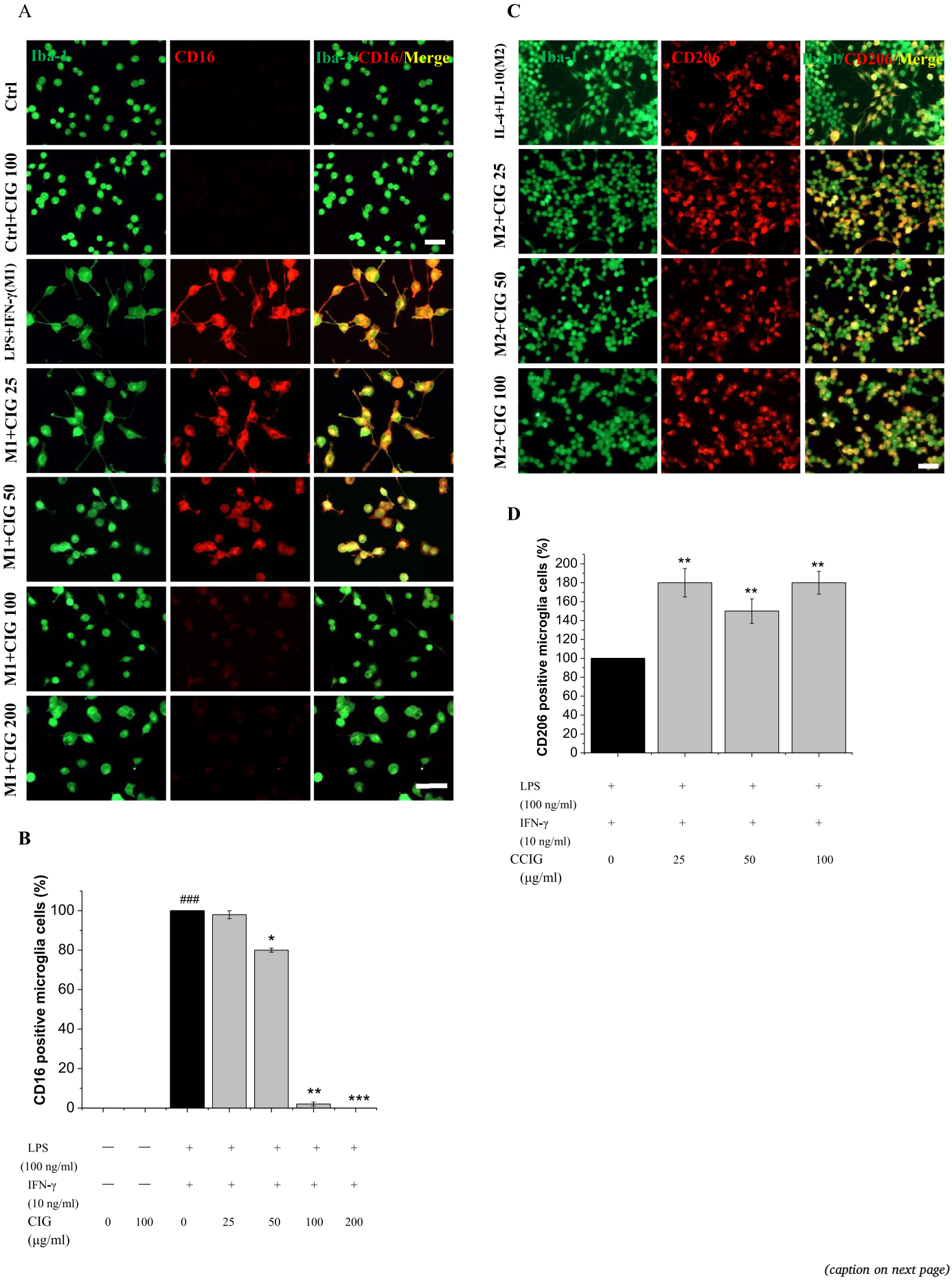

(caption on next page)

Fig. 3. Effect of cornel iridoid glycoside (CIG) on microglia polarization. (A) M1 microglia polarization induced by LPS/IFN-γ. Representative images of Iba-1 (green), CD16 (red) and Iba-1/CD16-dual label immunostaining in the BV2 cells. There is almost no red fluorescence in control (Ctrl) and Ctrl + 100 μg/mL group, whereas LPS/IFN-γ-treated cells showed obvious red fluorescence. CIG pretreatment for 24 h showed a decrease in red fluorescence, indicating an inhibition of M1 polarization. (B) Quantification of CD16 positive microglia cells. Values are the mean ± SEM from 3 independent experiments. (C) M2 microglia polarization induced by IL-4/IL-10. Representative images of Iba-1 (green), CD206 (red) and Iba-1/CD206-dual label immunostaining in the BV2 cells. IL-4/IL-10-treated cells showed obvious red fluorescence. CIG pretreatment for 24 h promoted or retained the red fluorescence, indicating an enhancement or maintenance of M2 polarization. (D) Quantification of CD206 positive microglia cells. Values are the mean ± SEM from 3 independent experiments. $^{*}P < .05$, $^{**}P < .01$, $^{***}P < .001$, significantly different from the LPS/IFN-γ-treated group; $^{\#\#\#}P < .001$ significantly different from the control group without LPS/IFN-γ stimulation. Representative images from at least three independent experiments are presented. Scale bar, 50 μm. (For interpretation of the references to colour in this figure legend, the reader is referred to the web version of this article.)

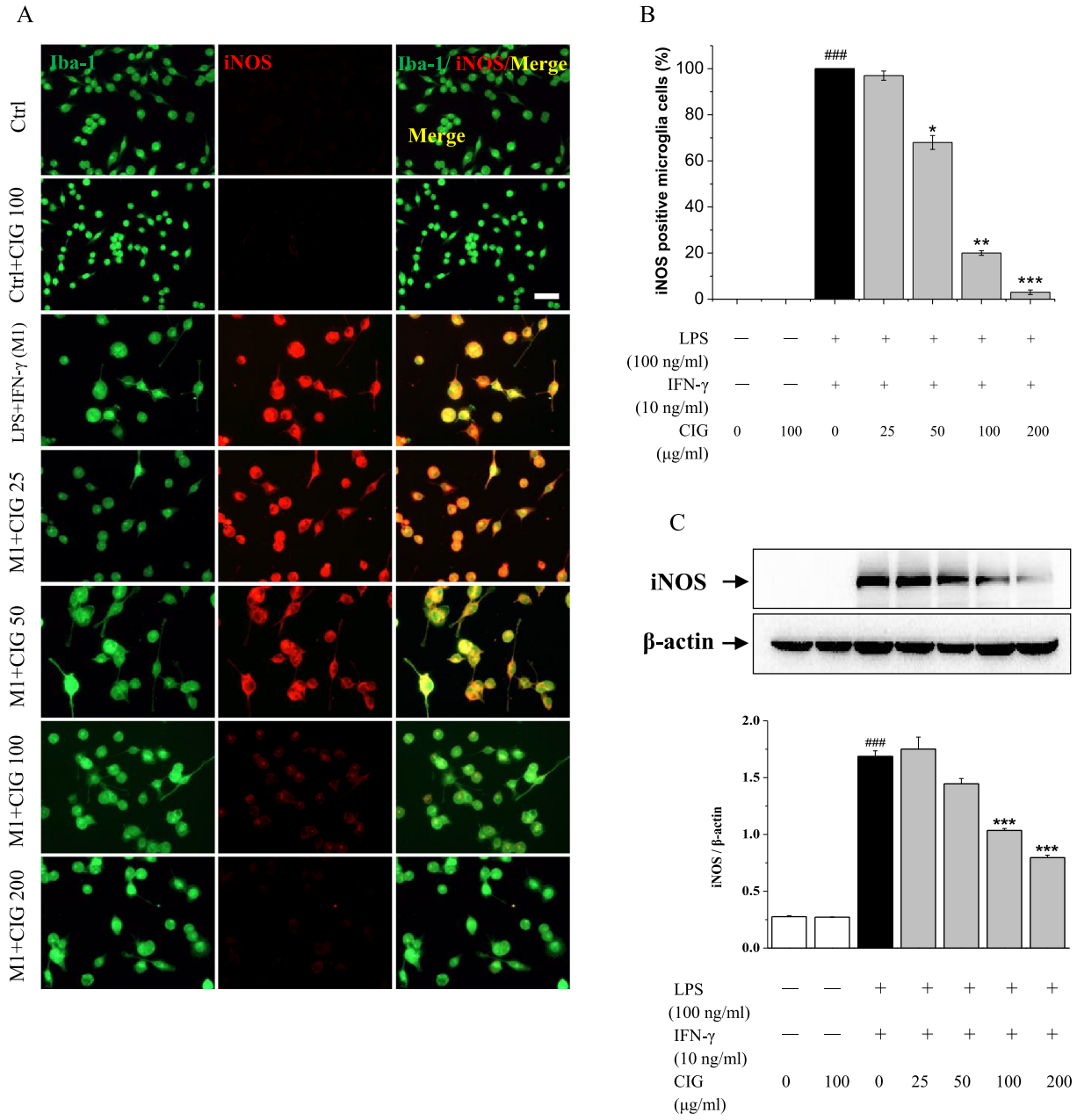

Fig. 4. Effects of cornel iridoid glycoside (CIG) on iNOS expression in LPS/IFN-γ-stimulated M1 microglia polarization. (A) Representative images of Iba-1 (green), iNOS (red) and Iba-1/iNOS-dual-label immunostaining in BV2 cells. There is almost no red fluorescence in the control (Ctrl) and Ctrl + 100 μg/mL groups, whereas LPS/IFN-γ-treated cells showed obvious red fluorescence. CIG (100 and 200 μg/mL) pretreatment for 24 h showed a decrease in red fluorescence, indicating an inhibition of iNOS expression. (B) Quantification of iNOS positive microglia cells. (C) Cell extracts were prepared from the BV2 cells and were immunoblotted with the indicated Abs. The level of iNOS protein was normalized with β-actin that was arbitrarily set to 100%. Quantification of western blot data (lower panel). Values are the mean ± SEM from 3 independent experiments. $^{*}P < .05$, $^{**}P < .01$, $^{***}P < .001$, significantly different from the LPS/IFN-γ-treated group; $^{\#\#\#}P < .001$ significantly different from the control group without LPS/IFN-γ stimulation. (For interpretation of the references to colour in this figure legend, the reader is referred to the web version of this article.)

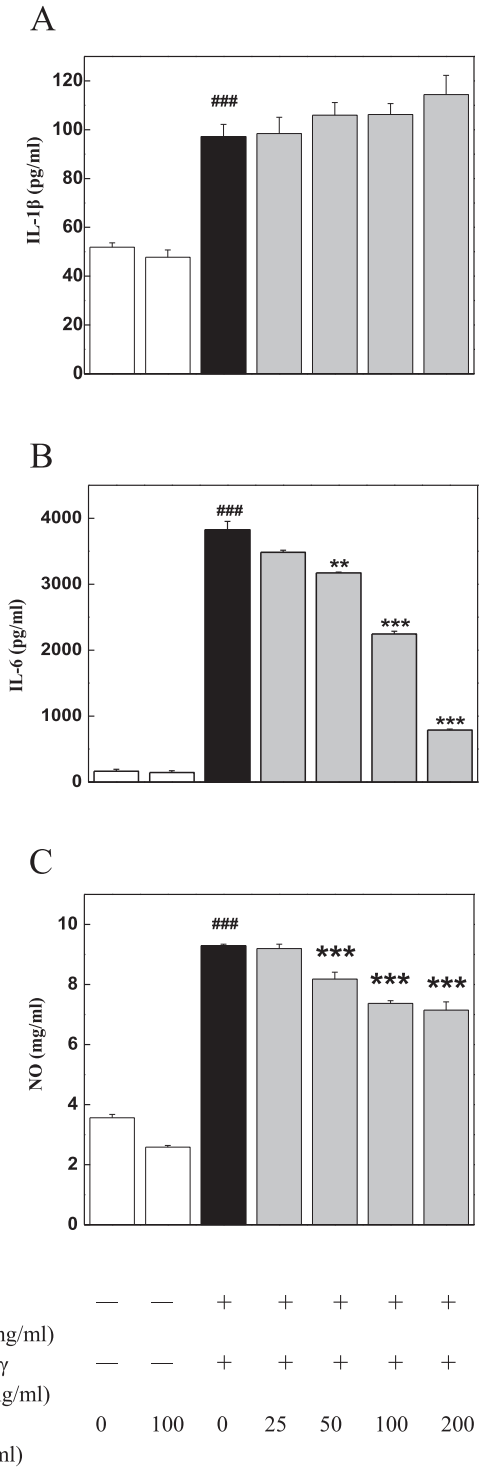

Fig. 5. Effects of cornel iridoid glycoside (CIG) on IL-1β (A), IL-6 (B) and NO (C) production in the LPS/IFN-γ-stimulated BV2 microglia cells. Cells were incubated with the indicated concentrations of CIG in the presence or absence of LPS (100 ng/mL)/IFN-γ (10 ng/mL) for 24 h, and the amounts of IL-1β, IL-6 and NO released into the media were determined. Data present as the mean ± SEM from 3 independent experiments performed in duplicate. $^{**}P < .01$, $^{***}P < .001$, significantly different from the LPS/IFN-γ-treated group; $^{###}P < .001$ significantly different from the control group without LPS/IFN-γ stimulation.

pathway.

The suppressors of cytokine signalling (SOCS) have been shown to regulate the responses of immune cells to cytokines (Kubo et al., 2003; Yoshimura et al., 2007). The discovery of the SOCS proteins suggested an important mechanism for the negative regulation of the cytokine-JAK/STAT pathway. Thus, we evaluated the effect of CIG on the expression of the SOCS1 protein induced by LPS/IFN-γ stimulation in the BV2 microglia cells. Our results demonstrated that CIG treatment could increase SOCS1 expression significantly, which may contribute to the inhibition of the JAK/STAT pathway (Fig. 7C).

3.8. Effects of CIG on NF-κB, COX-2 and ICAM-1 expression

NF-κB is a family of transcription factors central to immunity and inflammatory. It regulates expression of a number of genes including cytokines (Yin et al., 2012). Proinflammatory factor cyclooxygenase-2 (COX-2) has been reported to have particular relevance to inflammation (Yin et al., 2005). Intercellular adhesion molecule 1 (ICAM-1), one of the cell adhesion molecules covering the surface of endothelial cells, mediates the adhesion and extravasation of leukocytes and plays a pivotal role in the inflammatory response (Zhong et al., 2018). Therefore, the expression levels of NF-κB, COX-2 and ICAM-1 were examined. As shown in Fig. 9, a marked increase in NF-κB expression was observed after LPS/IFN-γ stimulation in the BV2 cells, while this increase was not significantly inhibited by CIG, as examined by immunoblotting analysis. LPS/IFN-γ induced COX-2 expression was inhibited markedly by CIG at a dose of 200 μg/mL. In addition, CIG (25, 50, 100 and 200 μg/mL) dose-dependently suppressed ICAM-1 protein expression, significantly at doses of 100 and 200 μg/mL.

3.9. Effect of CIG on the expression of IL-6 receptors, IL-6Rα and gp130

IL (interleukin)-6, a multifunctional cytokine that regulates the immune and inflammatory responses, has multiple biological activities through its unique receptor system. IL-6 exerts its biological activities through two molecules: IL-6R (IL-6 receptor) and gp130. When the IL-6-IL-6R complex is formed, homodimerization of gp130 is induced. The homodimerization of the receptor complex activates JAK phosphorylation (Mihara et al., 2012). Thus, the expression of IL-6 receptors IL-6R and gp130, upstream of the JAK/STAT pathway, were examined. As shown in Fig. 10, increased IL-6Rα and gp130 expression was induced obviously by the LPS/IFN-γ stimulation in BV2 cells; this increase was inhibited significantly by CIG at doses of 100 and 200 μg/mL examined by immunoblotting analysis.

3.10. CIG inhibited the interaction between LPS or IFN-γ with their receptors inside N9 microglial cells

We measured the ability of CIG to inhibit the interaction between LPS or IFN-γ with their intracellular receptors in N9 cells. When N9 cells were treated with Alex Fluor 488-conjugated LPS combined with Alexa Fluor 594-conjugated IFN-γ alone, the fluorescence intensity of LPS and IFN-γ was observed outside the cell membrane by confocal microscope analysis (Fig. 11). However, in the presence of CIG (100 μg/mL), the binding of Alexa Fluor 488-conjugated LPS and Alexa Fluor 594-conjugated IFN-γ to N9 cells was significantly inhibited. Minocycline (20 μM) served as a positive control. Thus, the inhibition of the interaction between LPS and IFN-γ with their intracellular receptors may be one of the possible mechanisms for the anti-inflammatory effects of CIG.

4. Discussion

In the present study, we demonstrated the anti-inflammatory effects of CIG on $MOG_{35–55}$-induced EAE, an animal model of MS, and analysed its underlying molecular mechanisms. CIG delayed the onset of EAE, ameliorated the severity of symptoms and inhibited the activation of the microglia in different brain regions such as the corpus callosum, lateral ventricles and optic tract of mice. In addition, CIG has

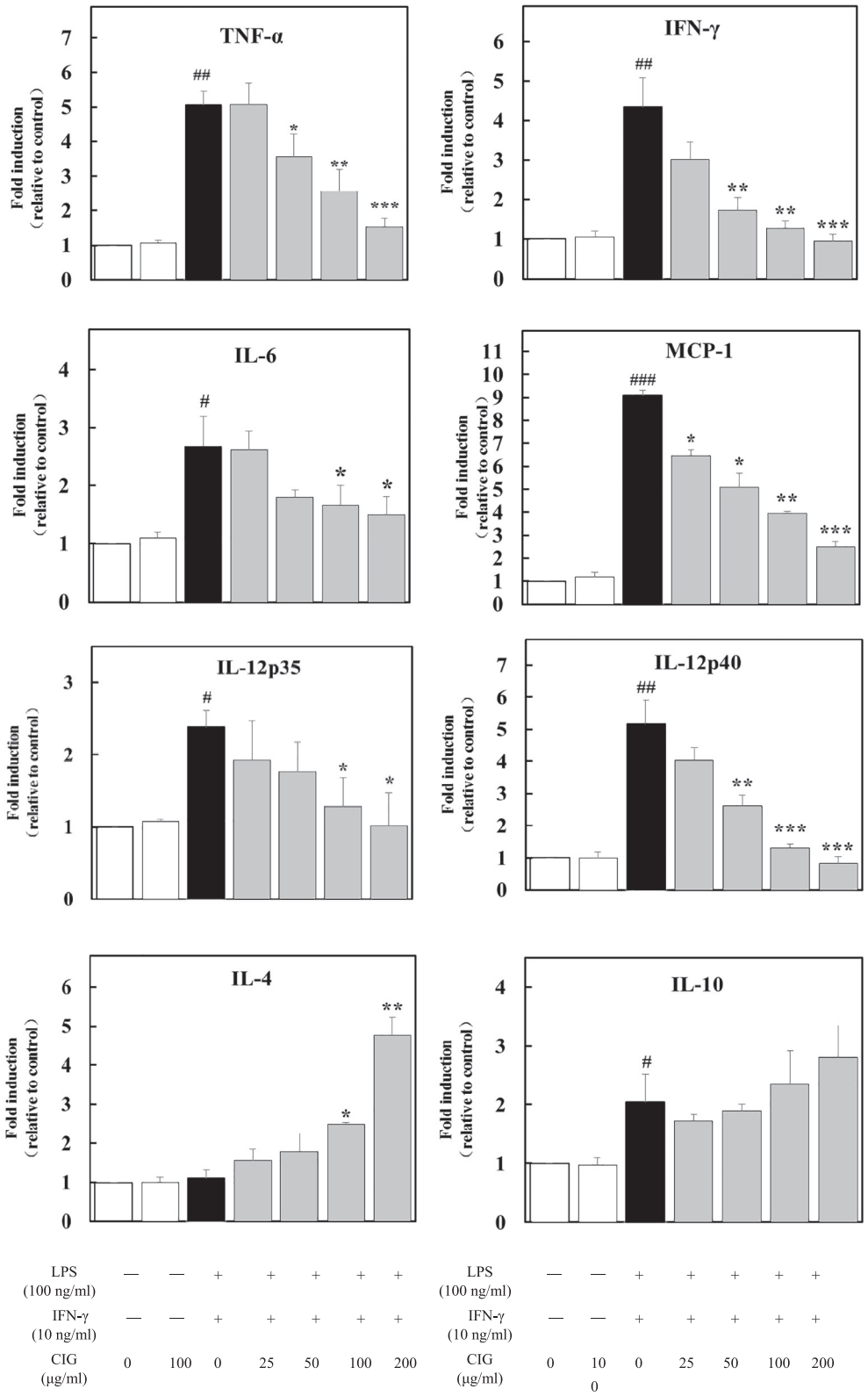

Fig. 6. Effects of cornel iridoid glycoside (CIG) on mRNA expression of various inflammatory mediators. Cells were collected after LPS/IFN-γ-stimulation for 24 h, which were pretreated with or without CIG for 30 min, and mRNA was analysed by real-time PCR for TNF-α, IFN-γ, IL-6, IL-12 (p35 and p40), IL-4, IL-10, and MCP-1. $^{*}P < .05$, $^{**}P < .01$, $^{***}P < .001$, significantly different from the LPS/IFN-γ-treated group; $^{\#}P < .05$, $^{\#\#}P < .01$ and $^{\#\#\#}P < .001$ significantly different from the control group without LPS/IFN-γ stimulation.

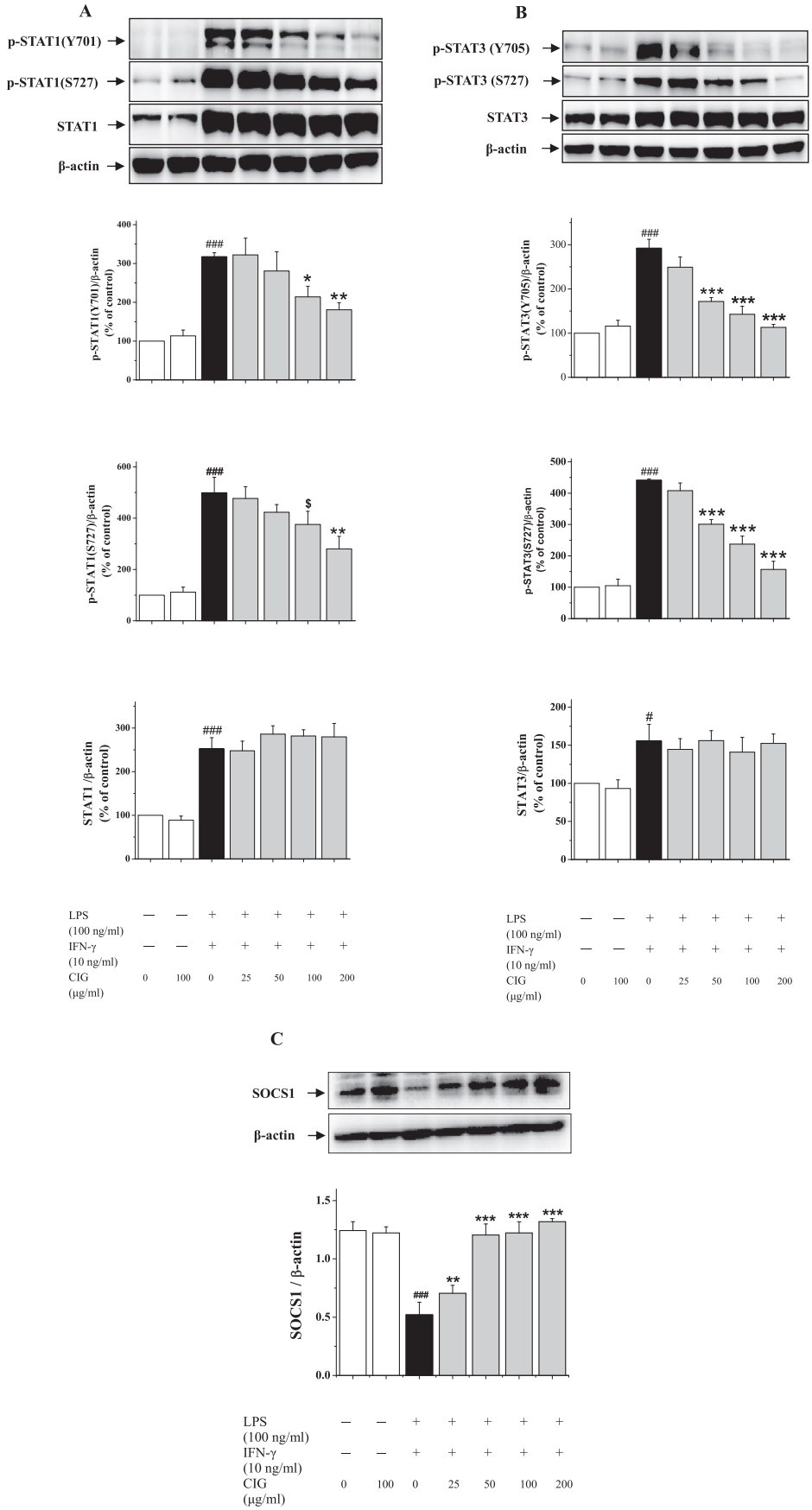

Fig. 7. Effects of cornel iridoid glycoside (CIG) on STAT1/STAT3 phosphorylation and its negative regulator SOCS1 in the LPS/IFN-γ-stimulated BV2 microglia cells. Cell extracts were prepared from BV2 cells and were immunoblotted with the indicated Abs. Levels of the active forms of STAT1, STAT3, and SOCS1 were normalized with β-actin and are expressed as fold changes versus the untreated control samples that were arbitrarily set to 100%. Quantification of western blot data (lower panel). Values are the mean ± SEM from 3 independent experiments. $^{\$}P = .053$, $^{*}P < .05$, $^{**}P < .01$, $^{***}P < .001$, significantly different from the LPS/IFN-γ-treated group; $^{\#}P < .05$, $^{\#\#\#}P < .001$ significantly different from the control group without LPS/IFN-γ stimulation.

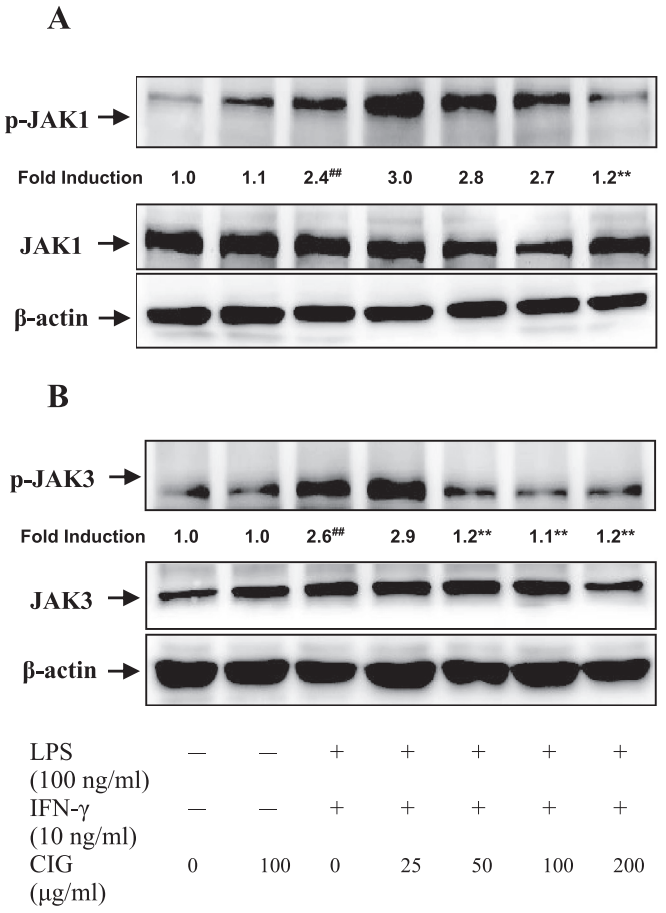

Fig. 8. Effects of cornel iridoid glycoside (CIG) on JAK1/JAK3 phosphorylation in the LPS/IFN-γ-stimulated BV2 microglia cells. Cell protein extracts were prepared from the BV2 cells and were immunoblotted with the indicated Abs. $^{**}P < .01$, significantly different from the LPS/IFN-γ-treated group; $^{\#\#}P < .01$ significantly different from the control group without LPS/IFN-γ stimulation.

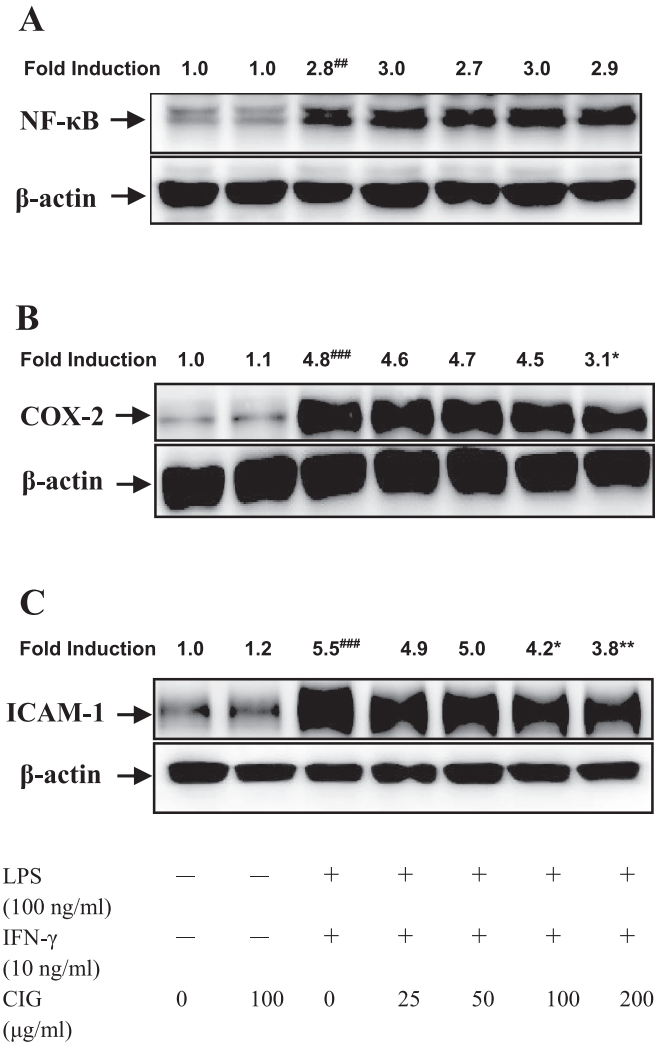

Fig. 9. Effects of cornel iridoid glycoside (CIG) on NF-κB, COX-2, ICAM-1 in the LPS/IFN-γ-stimulated BV2 microglia cells. Cell protein extracts were prepared from the BV2 cells and were immunoblotted with the indicated Abs. Representative image of three independent experiments is shown. β-actin was used as an internal control. $^{*}P < .05$, $^{**}P < .01$, significantly different from the LPS/IFN-γ-treated group; $^{\#\#}P < .01$, $^{\#\#\#}P < .001$ significantly different from the control group without LPS/IFN-γ stimulation.

therapeutic potential through the modulation of microglia polarization, which inhibits inflammatory responses towards the M1 phenotype and shifts to M2 in vitro. Triplicate independent EAE experiments were performed to examine the effect of CIG on $MOG_{35–55}$-induced EAE animal model. It seems that the group of EAE + CIG50 mice develop more severe EAE than EAE only. In fact, there is no significant difference between the two groups in the severity of neurological deficit.

MS is a debilitating T-cell-mediated autoimmune disease of the CNS (Fletcher et al., 2010). Infiltrating cells in the CNS during EAE are mainly composed of T cells and microglia cells. Adoptive transfer studies have established that T cells are both necessary and sufficient for induction of EAE (Meng et al., 2011). Microglia cells also play indispensable roles in the development of EAE (Yamasaki et al., 2014; Almolda et al., 2011). Microglia are generally considered the resident immune cells of the CNS that regulate the primary events of the neuroinflammatory response. Recent studies have revealed that microglia actively participate in the pathogenesis of EAE progression (Chu et al., 2018; Jiang et al., 2014; Yin et al., 2014). There are two main phenotypes that occur prominently in inflammatory lesions. LPS and IFN-γ induce microglia expression of proinflammatory cytokines and mediators, such as IL-1β and tumour necrosis factor-α (TNF-α). These "classically activated" microglia are defined as M1 microglia. M1 cells also express the cell surface marker CD16 and have iNOS activity. On the other hand, IL-4 and IL-10 promote "alternatively activated" M2 microglia differentiation. The M2 microglia cells are anti-inflammatory and induce tissue repair. The M2 subclass of microglia can be identified by the expression of the mannose receptor (CD206) as well as the enzyme arginase 1 (Arg1). The most important result in this study is that CIG treatment reduced the numbers of $Iba1^+/CD16^+$ M1 microglia and increased or maintained the numbers of $Iba1^+/CD206^+$ M2 microglia in vitro (Gao and Tsirka, 2011; Rawji and Yong, 2013).

The imbalance of M1/M2 microglia is a key factor in the severity of inflammation and has been confirmed in relapsing EAE in rats (Mikita et al., 2011). Based on a large amount of literature in the field of microglia polarization, we selected the markers of M1 polarization, such as IL-1β, IL-6, NO, TNF-α, IFN-γ, IL-12 and MCP-1, as well as the markers of M2 polarization, such as IL-4 and IL-10, to analyse in our study. Our data demonstrated that CIG could inhibit M1 cytokine release and mRNA expression, and promote expression of M2 cytokines such as IL-4 and IL-10 as examined by ELISA or real-time PCR, suggesting CIG shifts M1 microglia to the M2 phenotype. However, only microglia cell lines were used in this study. Data obtained from primary microglia and animal model will show in the future.

JAKs, STATs and SOCS proteins are associated with human autoimmune diseases, especially pathways leading to STAT1 and STAT3 activation (Kutty et al., 2010; Villarino et al., 2015, 2017). JAK/STAT

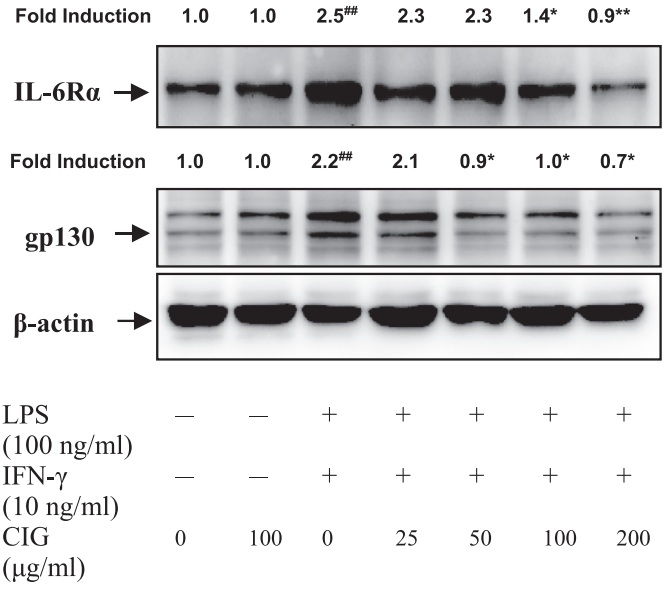

Fig. 10. Effects of cornel iridoid glycoside (CIG) on the protein levels of IL-6 receptors, IL-6Rα and gp130 examined by western blotting analysis. Cell protein extracts were prepared from the BV2 cells and were immunoblotted with the indicated Abs. Representative image of three independent experiments is shown. β-actin was used as an internal control. $^{*}P < .05$, $^{**}P < .01$, significantly different from the LPS/IFN-γ-treated group; $^{\#\#}P < .01$, significantly different from the control group without LPS/IFN-γ stimulation.

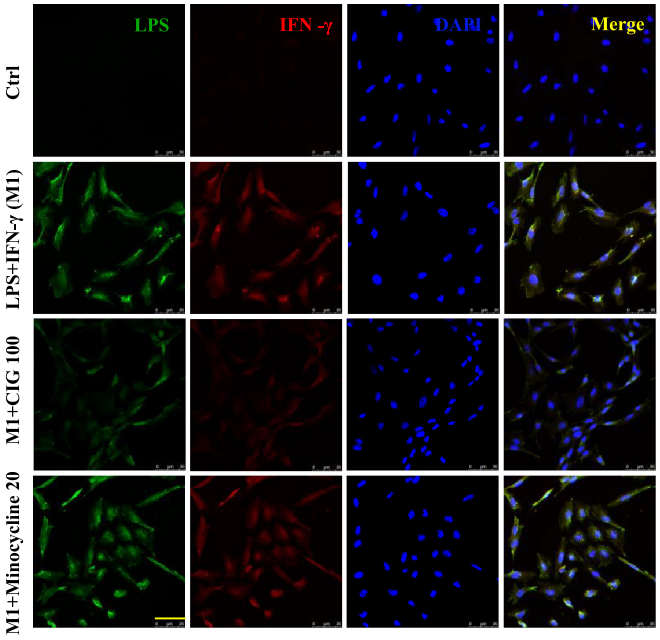

Fig. 11. Inhibitory effect of cornel iridoid glycoside (CIG) on the intracellular receptors of LPS or IFN-γ in N9 microglia cells by confocal microscope analysis. The N9 cells were incubated with CIG (100 μg/mL) or minocycline (20 μM) for 30 min and then treated with Alexa Fluor 488-conjugated LPS combined with Alexa Fluor 594-conjugated IFN-γ for 24 h. The cells were fixed with 4% formaldehyde, incubated with DAPI and then analysed by confocal microscope.

signalling begins with the extracellular association of cytokines or growth factors with their corresponding transmembrane receptors. This facilitates trans-activation of the receptor-bound JAKs by putting them in spatial proximity and by prompting conformational changes that distance their kinase domains from inhibitory pseudokinase domains (Brooks et al., 2014). Activated JAKs then phosphorylate latent STAT monomers, leading to dimerization, nuclear translocation, and DNA binding. In mammals, four JAKs (JAK1, JAK2, JAK3, TYK2) and seven STATs (STAT1, STAT2, STAT3, STAT4, STAT5a, STAT5b, STAT6) are used by > 50 cytokines and growth factors (Villarino et al., 2015). Given the data implicating JAK/STAT in autoimmune disease, this pathway has become an attractive target for pharmaceuticals. Ruxolitinib, a JAK1 and JAK2 inhibitor, has shown efficacy for the treatment of polycythemia vera and myelofibrosis. Tofacitinib, a JAK3 inhibitor, was the first drug for rheumatoid arthritis approved by U.S. Food and Drug Administration. AZD1480, a specific inhibitor of the JAK/STAT pathway, showed a striking beneficial immunomodulatory effect in five different models of EAE (Liu et al., 2014). Two herbal compounds, plumbagin and berberine, have been reported to ameliorate EAE through downregulation of the JAK/STAT signalling pathway (Jia et al., 2011). In our previous study, we have reported that the JAK/STAT signalling pathway is involved in the effect of CIG in $MBP_{68–86}$-induced EAE rats. To elucidate the precise mechanism of CIG, the activation of the JAK/STAT signalling pathway was examined in vitro. Our results demonstrated that CIG inhibited the phosphorylation of STAT1 (Y701 and S727), STAT3 (Y705 and S727), JAK1 and JAK3 in activated microglia. Qin et al. (2012b) reported that mice with conditional knockout of SOCS in cells of the myeloid lineage develop a severe neurological deficit with features of EAE, which is associated with hyperactivation of the JAK/STAT signalling pathway in the CNS (Qin et al., 2012a,b). CIG pretreatment increased SOCS1 expression significantly. Thus, inhibition of the JAK/STAT pathway and promotion of SOCS1 may be related to the therapeutic potential of CIG.

The JAK/STAT pathway was discovered 20 years ago as a mediator of cytokine signalling. Although there are dozens of cytokines and cytokine receptors, four JAKs, and seven STATs, it seems that IL-6-mediated activation of STAT3 is a principal pathway implicated in promoting MS or EAE (Benveniste et al., 2014; Cheon et al., 2011). IL-6 exerts its biological activities through two receptor molecules, IL-6R and gp130. Thus, the expression levels of the IL-6 receptors, IL-6R and gp130, upstream of JAK/STAT pathway, were examined. CIG pretreatment inhibited the increase of IL-6Rα and gp130 induced by LPS/IFN-γ stimulation in BV2 cells. Marked increases in NF-κB, COX-2 and ICAM-1 expression were observed after the LPS/IFN-γ stimulation in the BV2 cells, while these increases were not observed or moderately inhibited by CIG pretreatment.

LPS, a constituent of gram-negative bacteria, binds to TLR4 and evokes intracellular inflammatory signalling cascades including interleukin-1 receptor-associated kinase, NF-κB and MAPKs activation (Lu et al., 2008). The IFN-γ receptor complex consists of two chains: IFN-γR1, the ligand-binding chain, and IFN-γR2, the accessory chain. Binding of IFN-γ causes oligomerization of the two IFN-γ receptor subunits, IFN-γR1 and IFN-γR2, which initiates the following signal transduction events: activation of JAK1 and JAK2 receptor-associated protein tyrosine kinases, phosphorylation of the IFN-γR1 intracellular domain on Tyr440 followed by phosphorylation and activation of STAT1α (Pestka et al., 1997). In the present study, we demonstrated that CIG inhibits LPS or IFN-γ binding to intracellular receptors, indicating the antagonistic effect of CIG against TLR4 or IFN-γR. Therefore, the antagonistic function of CIG against TLR4 or IFN-γR may be responsible for the anti-inflammatory effects or the JAK/STAT signalling pathway inhibition in the LPS/IFN-γ-stimulated microglia.

5. Conclusions

CIG delays onset and ameliorates severity of EAE in mice, accompanied by inhibition of inflammation. Interestingly, CIG shifts microglia from the M1 to the M2 phenotype, producing less inflammatory cytokines. In addition, CIG pre-treatment significantly prevented JAK/STAT signalling pathway activation in LPS/IFN-γ-stimulated microglia. The suppression of LPS or IFN-γ binding to their intracellular receptors may play a pivotal role in the effect of CIG. Based on our findings, CIG might

be a promising candidate for preventing neurological disorders such as MS. However, the exact function of CIG in the treatment of MS still merits further investigation.

Competing interests

The authors declare no competing financial interests.

Fundings

This work was supported by the Beijing Natural Science Foundation (7162208), Beijing Health and Technical Personal of High-level Plan (No. 2014-3-052), National Natural Science Foundation of China (No. 81473740, No. 81673627), Guangzhou Science Technology and Innovation Commission Technology Research Projects (201805010005), Beijing Municipal Administration of Hospitals Incubating Program (PZ2016027) and Youth Programme of Beijing Municipal Administration of Hospitals' (QML20160805).

References

Ahn, Y.H., Jeon, S.B., Chang, C.Y., Goh, E.A., Kim, S.S., Kim, H.J., Song, J., Park, E.J., 2017. Glatiramer acetate attenuates the activation of CD4+ T cells by modulating STAT1 and −3 signaling in glia. Sci. Rep. 7, 40484.

Almolda, B., Gonzalez, B., Castellano, B., 2011. Antigen presentation in EAE: role of microglia, macrophages and dendritic cells. Front. Biosci. (Landmark Ed). 16, 1157–1171.

Benveniste, E.N., Liu, Y., McFarland, B.C., Qin, H., 2014. Involvement of the janus kinase/signal transducer and activator of transcription signaling pathway in multiple sclerosis and the animal model of experimental autoimmune encephalomyelitis. J. Interf. Cytokine Res. 34, 577–588.

Brooks, A.J., Dai, W., O'Mara, M.L., Abankwa, D., Chhabra, Y., Pelekanos, R.A., Gardon, O., Tunny, K.A., Blucher, K.M., Morton, C.J., Parker, M.W., Sierecki, E., Gambin, Y., Gomez, G.A., Alexandrov, K., Wilson, I.A., Doxastakis, M., Mark, A.E., Waters, M.J., 2014. Mechanism of activation of protein kinase JAK2 by the growth hormone receptor. Science 344, 1249783.

Cheon, H., Yang, J., Stark, G.R., 2011. The functions of signal transducers and activators of transcriptions 1 and 3 as cytokine-inducible proteins. J. Interf. Cytokine Res. 31, 33–40.

Chu, F., Shi, M., Zheng, C., Shen, D., Zhu, J., Zheng, X., Cui, L., 2018. The roles of macrophages and microglia in multiple sclerosis and experimental autoimmune encephalomyelitis. J. Neuroimmunol. 318, 1–7.

Fletcher, J.M., Lalor, S.J., Sweeney, C.M., Tubridy, N., Mills, K.H., 2010. T cells in multiple sclerosis and experimental autoimmune encephalomyelitis. Clin. Exp. Immunol. 162, 1–11.

Gao, Z., Tsirka, S.E., 2011. Animal models of MS reveal multiple roles of microglia in disease pathogenesis. Neurol. Res. Int. 2011, 383087.

Gilgun-Sherki, Y., Panet, H., Melamed, E., Offen, D., 2003. Riluzole suppresses experimental autoimmune encephalomyelitis: implications for the treatment of multiple sclerosis. Brain Res. 989, 196–204.

Harry, G.J., 2013. Microglia during development and aging. Pharmacol. Ther. 139, 313–326.

Hu, X., Leak, R.K., Shi, Y., Suenaga, J., Gao, Y., Zheng, P., Chen, J., 2015. Microglial and macrophage polarization—new prospects for brain repair. Nat. Rev. Neurol. 11, 56–64.

Jia, Y., Jing, J., Bai, Y., Li, Z., Liu, L., Luo, J., Liu, M., Chen, H., 2011. Amelioration of experimental autoimmune encephalomyelitis by plumbagin through down-regulation of JAK-STAT and NF-κB signaling pathways. PLoS One 6, e27006.

Jiang, Z., Jiang, J.X., Zhang, G.X., 2014. Macrophages: a double-edged sword in experimental autoimmune encephalomyelitis. Immunol. Lett. 160, 17–22.

Jung, J.S., Shin, K.O., Lee, Y.M., Shin, J.A., Park, E.M., Jeong, J., Kim, D.H., Choi, J.W., Kim, H.S., 2013. Anti-inflammatory mechanism of exogenous C2 ceramide in lipopolysaccharide-stimulated microglia. Biochim. Biophys. Acta 1831, 1016–1026.

Kubo, M., Hanada, T., Yoshimura, A., 2003. Suppressors of cytokine signaling and immunity. Nat. Immunol. 4, 1169–1176.

Kutty, R.K., Nagineni, C.N., Samuel, W., Vijayasarathy, C., Hooks, J.J., Redmond, T.M., 2010. Inflammatory cytokines regulate microRNA-155 expression in human retinal pigment epithelial cells by activating JAK/STAT pathway. Biochem. Biophys. Res. Commun. 402, 390–395.

Liu, Y., Holdbrooks, A.T., De Sarno, P., Rowse, A.L., Yanagisawa, L.L., McFarland, B.C., Harrington, L.E., Raman, C., Sabbaj, S., Benveniste, E.N., Qin, H., 2014. Therapeutic efficacy of suppressing the Jak/STAT pathway in multiple models of experimental autoimmune encephalomyelitis. J. Immunol. 192, 59–72.

Lu, Y.C., Yeh, W.C., Ohashi, P.S., 2008. LPS/TLR4 signal transduction pathway. Cytokine 42, 145–151.

Mendel, I., Katz, A., Kozak, N., Ben-Nun, A., Revel, M., 1998. Interleukin-6 functions in autoimmune encephalomyelitis: a study in gene-targeted mice. Eur. J. Immunol. 28, 1727–1737.

Meng, L., Ouyang, J., Zhang, H., Wen, Y., Chen, J., Zhou, J., 2011. Treatment of an autoimmune encephalomyelitis mouse model with nonmyeloablative conditioning and syngeneic bone marrow transplantation. Restor. Neurol. Neurosci. 29, 177–185.

Meng, S., Zhou, G., Gu, Q., Chanda, P.K., Ospino, F., Cooke, J.P., 2016. Transdifferentiation requires iNOS activation role of RING1A S-nitrosylation. Circ. Res. 119, e129–e138.

Mihara, M., Hashizume, M., Yoshida, H., Suzuki, M., Shiina, M., 2012. IL-6/IL-6 receptor system and its role in physiological and pathological conditions. Clin. Sci. (Lond). 122, 143–159.

Mikita, J., Dubourdieu-Cassagno, N., Deloire, M.S., Vekris, A., Biran, M., Raffard, G., Brochet, B., Canron, M.H., Franconi, J.M., Boiziau, C., Petry, K.G., 2011. Altered M1/M2 activation patterns of monocytes in severe relapsing experimental rat model of multiple sclerosis. Amelioration of clinical status by M2 activated monocyte administration. Mult. Scler. J. 17, 2–15.

Miron, V.E., Boyd, A., Zhao, J.W., Yuen, T.J., Ruckh, J.M., Shadrach, J.L., van Wijngaarden, P., Wagers, A.J., Williams, A., Franklin, R.J.M., Ffrench-Constant, C., 2013. M2 microglia and macrophages drive oligodendrocyte differentiation during CNS remyelination. Nat. Neurosci. 16, 1211–1218.

Ogata, H., Kobayashi, T., Chinen, T., Takaki, H., Sanada, T., Minoda, Y., Koga, K., Takaesu, G., Maehara, Y., Iida, M., Yoshimura, A., 2006. Deletion of the SOCS3 gene in liver parenchymal cells promotes hepatitis-induced hepatocarcinogenesis. Gastroenterology 131, 179–193.

O'Loughlin, E., Madore, C., Lassmann, H., Butovsky, O., 2018. Microglial phenotypes and functions in multiple sclerosis. Cold Spring Harb. Perspect. Med. 8 (pii), a028993.

O'Shea, J.J., Plenge, R., 2012. JAK and STAT signaling molecules in immunoregulation and immune-mediated disease. Immunity 36, 542–550.

Pestka, S., Kotenko, S.V., Muthukumaran, G., Izotova, L.S., Cook, J.R., Garotta, G., 1997. The interferon gamma (IFN-gamma) receptor: a paradigm for the multichain cytokine receptor. Cytokine Growth Factor Rev. 8, 189–206.

Qin, X., Guo, B.T., Wan, B., Fang, L., Lu, L., Wu, L., Zang, Y.Q., Zhang, J.Z., 2010. Regulation of Th1 and Th17 cell differentiation and amelioration of experimental autoimmune encephalomyelitis by natural product compound berberine. J. Immunol. 18, 1855–1863.

Qin, H., Holdbrooks, A.T., Liu, Y., Reynolds, S.L., Yanagisawa, L.L., Benveniste, E.N., 2012a. SOCS3 deficiency promotes M1 macrophage polarization and inflammation. J. Immunol. 189, 3439–3448.

Qin, H., Yeh, W.I., De Sarno, P., Holdbrooks, A.T., Liu, Y., Muldowney, M.T., Reynolds, S.L., Yanagisawa, L.L., Fox 3rd, T.H., Park, K., Harrington, L.E., Raman, C., Benveniste, E.N., 2012b. Signal transducer and activator of transcription-3/suppressor of cytokine signaling-3 (STAT3/SOCS3) axis in myeloid cells regulates neuroinflammation. Proc. Natl. Acad. Sci. U. S. A. 109, 5004–5009.

Rawji, K.S., Yong, V.W., 2013. The benefits and detriments of macrophages/microglia in models of multiple sclerosis. Clin. Dev. Immunol. 2013, 948976.

Stromnes, I.M., Goverman, J.M., 2006. Active induction of experimental allergic encephalomyelitis. Nat. Protoc. 1, 1810–1819.

Tremblay, M.È., Stevens, B., Sierra, A., Wake, H., Bessis, A., Nimmerjahn, A., 2011. The role of microglia in the healthy brain. J. Neurosci. 31, 16064–16069.

Villarino, A.V., Kanno, Y., Ferdinand, J.R., O'Shea, J.J., 2015. Mechanisms of Jak/STAT signaling in immunity and disease. J. Immunol. 194, 21–27.

Villarino, A.V., Kanno, Y., O'Shea, J.J., 2017. Mechanisms and consequences of Jak-STAT signaling in the immune system. Nat. Immunol. 18, 374–384.

Yamasaki, R., Lu, H., Butovsky, O., Ohno, N., Rietsch, A.M., Cialic, R., Wu, P.M., Doykan, C.E., Lin, J., Cotleur, A.C., Kidd, G., Zorlu, M.M., Sun, N., Hu, W., Liu, L., Lee, J.C., Taylor, S.E., Uehlein, L., Dixon, D., Gu, J., Floruta, C.M., Zhu, M., Charo, I.F., Weiner, H.L., Ransohoff, R.M., 2014. Differential roles of microglia and monocytes in the inflamed central nervous system. J. Exp. Med. 211, 1533–1549.

Yao, R.Q., Zhang, L., Wang, W., Li, L., 2009. Cornel iridoid glycoside promotes neurogenesis and angiogenesis and improves neurological function after focal cerebral ischemia in rats. Brain Res. Bull. 79, 69–76.

Yin, L.L., Zhang, W.Y., Li, M.H., Shen, J.K., Zhu, X.Z., 2005. CC 05, a novel anti-inflammatory compound, exerts its effect by inhibition of cyclooxygenase-2 activity. Eur. J. Pharmacol. 520, 172–178.

Yin, L.L., Lin, L.L., Zhang, L., Li, L., 2012. Epimedium flavonoids ameliorate experimental autoimmune encephalomyelitis in rats by modulating neuroinflammatory and neurotrophic responses. Neuropharmacology 63, 851–862.

Yin, L., Chen, Y., Qu, Z., Zhang, L., Wang, Q., Zhang, Q., Li, L., 2014. Involvement of JAK/STAT signaling in the effect of cornel iridoid glycoside on experimental autoimmune encephalomyelitis amelioration in rats. J. Neuroimmunol. 274, 28–37.

Yoshimura, A., Naka, T., Kubo, M., 2007. SOCS proteins, cytokine signalling, and immune regulation. Nat. Rev. Immunol. 7, 454–465.

Zhong, L., Simard, M.J., Huot, J., 2018. Endothelial microRNAs regulating the NF-κB pathway and cell adhesion molecules during inflammation. FASEB J. 32, 4070–4084.